Mat. Res. Bull. Vol. 3, pp. 471-482, 1968. Pergamon Press, Inc. Printed in the United States.

BAND ANTIFERROMAGNETISM AND THE NEW PEROVSKITE $CaCrO_3$

J. B. Goodenough, J. M. Longo, and J. A. Kafalas
Lincoln Laboratory, * Massachusetts Institute of Technology
Lexington, Massachusetts 02173

(Received April 23, 1968; Communicated by J. B. Goodenough)

ABSTRACT

The perovskite $CaCrO_3$ has been prepared by the solid-state reaction of CaO and CrO_2 at 65 kbar and 700°C. It has the O-orthorhombic structure with a = 5.287Å, b = 5.316Å, and c = 7.486Å. Below T_N = 90°K, it exhibits a parasitic ferromagnetism with σ_o = 0.295 emu/gm at 4.2°K. Up to 6 kbar, the pressure dependence of T_N gives dT_N/dP = -0.23°K/kbar. Four-probe resistivity measurements on a polycrystalline bar give resistivities of 10^6 and 10^4 ohm-cm at 77 and 300°K. Comparison with the properties of other ABO_3 perovskites having B = Mo^{4+}, Cr^{4+}, V^{3+} indicates that $CaCrO_3$ represents spontaneous collective-electron magnetism.

Introduction

Transition-metal oxides ABO_3 having the perovskite structure provide an isostructural set of compounds that are important for studying the change from localized to collective d electrons [1]. The perovskites $A^{2+}MoO_3$, $A^{2+}CrO_3$, $A^{3+}VO_3$ are significant because they each contain two d electrons per molecule while their properties vary from metallic with Pauli paramagnetism to semiconducting with spontaneous magnetism and crystallographic distortions characteristic of localized electrons. This means that, without varying the number of outer d electrons, we can study the transition from collective d electrons having no spontaneous magnetism to localized d electrons.

This paper reports the preparation and some properties of the new perovskite $CaCrO_3$, which belongs to this series, and compares these properties with those of the other members and with a phenomenological description of the localized-electron to collective-electron transition.

* Operated with support from the United States Air Force

Experimental

The existence of Cr^{4+} in solid state compounds is not common and, in most cases, is synthesized only at high pressures. In known Cr^{4+}-containing compounds that do not require high-pressure synthesis, the ratio of alkaline-earth cation to Cr^{4+} ion is greater than one (i.e. Sr_2CrO_4, Ba_2CrO_4, and Ba_3CrO_5). Two cubic perovskites containing Cr^{4+} cations have previously been prepared under high pressure: antiferromagnetic, semiconducting $PbCrO_3$ [2] and metallic, Pauli paramagnetic $SrCrO_3$ [3].

We have prepared $CaCrO_3$ by the solid state reaction of CaO and CrO_2 at 65 kbar and 700°C for 15 mins. The CaO was prepared by decomposition of $CaCO_3$ while the CrO_2 was prepared by the decomposition of CrO_3 at 400°C and 20 kbars. It was found necessary to dry the reactants at 100°C and quickly transfer them after weighing to a nitrogen-filled glove bag. To ensure complete reaction, the reactants were ground together in the glove bag (agate mortar and pestle) and loaded tightly into a cylindrical gold liner (4 mm dia x 10 mm) with gold end plugs. For reactions above 1000°C, platinum liners and end plugs were used. The samples were subjected to the desired pressure before the temperature was raised. After completion of the run, the sample was quenched by shutting off the power to the furnace. When the sample reached room temperature (about 1 min), the pressure was released and the sample examined with a Norelco X-ray powder diffractometer using CuKα radiation. The temperature of reaction was determined from a watts vs temperature plot that had previously been established with a thermocouple inserted into the cell.

The product of stoichiometric reaction always included varying amounts of Cr_2O_3, which could not be removed by washing. However, a small excess of CaO (5-10%) almost completely eliminated the Cr_2O_3 impurity, and the CaO impurity could be washed out with dilute acid. The Cr_2O_3 impurity most likely arises from local pressure variations or chemical inhomogeneities, both of which may cause CrO_2 to lose oxygen before it reacts with the CaO present. This same impurity problem has been reported by DeVries and Roth [4] in the preparation of $PbCrO_3$. When CaO was reacted with CrO_3 instead of CrO_2, the yellow Cr^{6+} compound $CaCrO_4$ was always formed. This compound was extremely stable and did not lose oxygen to form a perovskite phase up to 1200°C and 65 kbar. This is in contrast with $PbCrO_4$, which at 1300°C and 60 kbar gave mostly $PbCrO_3$ [4].

Thermogravimetric analysis was performed on a washed sample of $CaCrO_3$ which was reduced in a stream of H_2/Ar (15%) at 1000°C to CaO and Cr_2O_3. Experimental weight loss was 5.98% and is to be compared to the theoretical loss of 5.71%.

The x-ray powder diffraction pattern of $CaCrO_3$ could be completely indexed on the basis of an orthorhombic unit cell containing four formula units: ($\underline{a}$ = 5.287Å, $\underline{b}$ = 5.316Å, $\underline{c}$ = 7.486Å). The intensities are also in good agreement with those calculated for this orthorhombic cell. The type and degree of distortion from cubic symmetry are assumed to be those described by Geller [5] for $GdFeO_3$ (space group Pbnm). A comparison of observed and calculated intensities and interplanar spacings is given in Table 1. This type of distortion, which reduces the nearest-neighbor anion coordination of the A cation from 12 to 9+3, is found in every other known perovskite $CaBO_3$ (B = Ti, V, Mn, Mo, Ru) and appears to be due to the relatively small size of the Ca^{2+} ion (ionic radius ≈ 0.98Å) and the existence of covalent character in the Ca-O bond.

A resistivity of 1.4×10^4 ohm-cm at 300°K and 1.1×10^6 ohm-cm at 77°K was obtained by the four-probe Van de Pauw method in a dense cylinder (2 mm dia. x 1 mm) taken from a pressure run. This indicates that the sample is semiconducting rather than metallic.

Magnetic susceptibility χ_m was obtained with a vibrating-sample magnetometer and samples weighing about 200 mg. The material was studied in the temperature range $4.2 < T < 300$°K and in magnetic fields up to 17.2 kOe. A nickel standard was used to calibrate the instrument. Figure 1(a) shows $1/\chi_m$ vs T for $CaCrO_3$ in a field of 10 kOe. Parasitic ferromagnetism appears below the antiferromagnetic Néel temperature $T_N = 90$°K. Such parasitic ferromagnetism is a characteristic of the orthorhombic perovskites. Figure 1(b) displays the magnetization σ vs applied magnetic field H_a for three different temperatures. Below T_N, the magnetization obeys the usual formula for parasitic ferromagnetism:

$$\sigma = \sigma_o + \chi_m H_a \qquad (1)$$

giving σ_o = 0.22, 0.295 emu/gm at 77 and 4.2°K, respectively.

TABLE 1

X-Ray Data for $CaCrO_3$

HKL	d_{obs}	I_{obs}	I_{calc}	HKL	d_{obs}	I_{obs}	I_{calc}
110, 002	3.738	M	13	233, 125, 323, 215, 411	1.265	VW	2
111	3.338	VW	6				
020, 112, 200	2.646	VVS	100	042, 134, 330	1.250	VW	4
021, 201	2.489	VW	2	006, 314, 402	1.247	VW	1
120, 210	2.370	VW	1	240, 332, 116, 420	1.184	M	9
121	2.264	VW	1				
211, 103	2.255	W	5	135, 333	1.173	VW	3
022, 202	2.160	W	3	315	1.170	VW	1
113	2.076	VW	3	044	1 083	W	1
122, 212	2.003	VW	2	404	1.080	W	3
220, 004	1.872	VS	43	152	1.004	W	1
023, 221	1.816	W	4	244, 136	1.002	W	3
130, 222, 114, 310	1.674	W	9	424, 316, 512	1.000	M	9
				440	0.937	VW	1
131, 311	1.638	W	7	008	0.935	VW	1
132, 024, 204, 312	1.327	S	37	352	0.884	W	1
				336, 028, 532, 208, 600	0.883	M	12
133, 115, 313	1.391	VW	2				
040	1.328	W	2	260	0.840	VW	< 1
224, 400	1.323	M	14	444	0.838	W	2
141	1.270	VW	< 1	228, 620	0.837	W	4

$\underline{a} = 5.287 \pm 0.004$Å $\quad \underline{b} = 5.316 \pm 0.004$Å $\quad \underline{c} = 7.486 \pm 0.005$Å

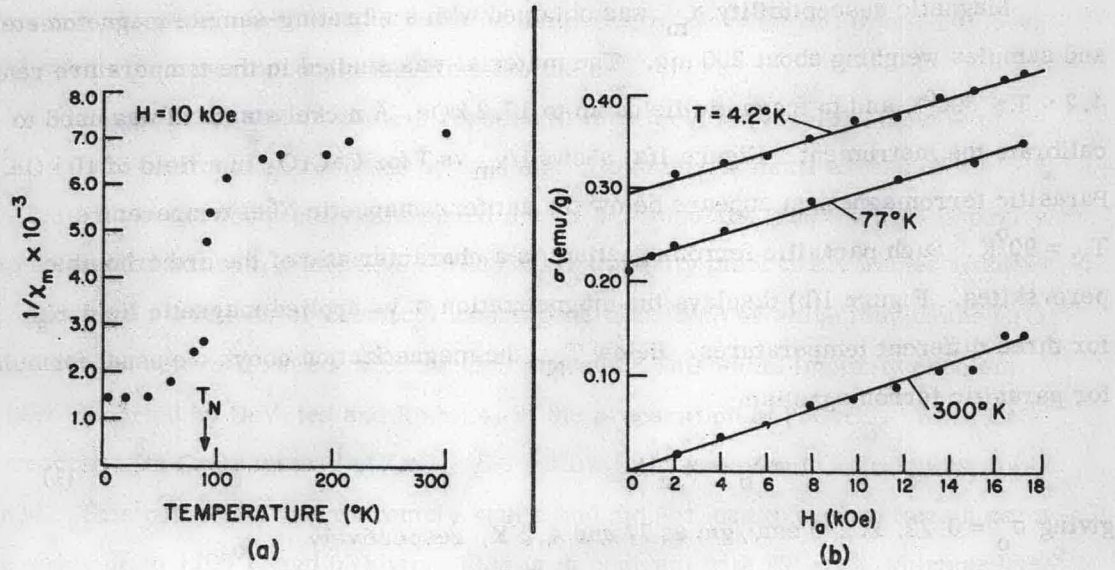

FIG. 1

Magnetic Properties of $CaCrO_3$

The effect of hydrostatic pressure on T_N was obtained from a vibrating-coil magnetometer equipped with a special pressure vessel made of a diamagnetic beryllium-copper alloy and using helium as the pressure-transmitting medium:

$$dT_N/dP = -0.23^{\circ}K/kbar \quad \text{up to 6 kbar} . \tag{2}$$

The Néel temperature was assumed to be given by the sharp increase with decreasing temperature in χ_m due to the appearance of parasitic ferromagnetism.

Phenomenological Phase Diagram

Localized d electrons are described by crystal-field theory. For a single electron outside closed-shell cores, the zero-order potential is spherical. This leads to wave functions of the form

$$f_{\ell m} = R_\ell(r)\, Y_\ell^m(\theta, \phi) \tag{3}$$

where $\ell = 2$ for outer d electrons. The spherical potential is perturbed by the cubic crystalline fields and by covalent mixing. Octahedral-site symmetry splits the atomic orbitals into the twofold-degenerate e_g orbitals directed toward near-neighbor anions and the more stable, threefold-degenerate t_{2g} orbitals directed toward near-neighbor A cations. After covalent mixing with the near-neighbor s and p orbitals, the crystal-field orbitals of e_g and t_{2g} symmetry are

$$\psi_e = N_\sigma(f_e + \lambda_\sigma \phi_\sigma) , \quad \psi_t = N_\pi(f_t + \lambda_\pi \phi_\pi + \lambda_A \phi_A) \tag{4}$$

where N_σ, N_π are normalization constants, λ_σ, λ_π, λ_A are covalent-mixing parameters, and ϕ_σ, ϕ_π, ϕ_A are the symmetrized anionic sp_σ, anionic p_π^2 and A-cationic sp^3 orbitals. (Covalent mixing with s, p orbitals on next-near-neighbor B cations would add a smaller fourth term to ψ_t.) Although the crystalline fields partially quench the orbital angular momentum, spin-orbit coupling splits the energy E_t of the states of t_{2g} symmetry into a more stable, four-fold degenerate (including spin) level $E_{3/2}$ and a less stable, two-fold degenerate level $E_{1/2}$, where

$$E_{1/2} - E_{3/2} = 2k_c\lambda \tag{5}$$

Here λ is the atomic parameter entering the spin-orbit-coupling energy $\lambda \underset{\sim}{L} \cdot \underset{\sim}{S}$, and k_c is a large fraction ($\sim$0.9) reflecting the increase in R(r) due to covalent mixing.

In the case of two, localized outer d electrons, intra-atomic exchange splits the states of different spin, α and β, and the ground state corresponds to the fivefold degenerate energy E_2 for states with total angular momentum $J = L + S = 2$, where

$$E_1 - E_2 = 3k_c\lambda \quad . \tag{6}$$

Interactions between near-neighbor B cations arise via the matrix elements

$$b_{ij} \equiv (\psi_i, h\psi_j) \approx \epsilon(\psi_i, \psi_j) \sim \epsilon N_\pi^2 \lambda_\pi^2 \tag{7}$$

where h is the change in the localized-electron potential energy of the B cation at $\underset{\sim}{R}_i$ that is due to the presence of a B cation at $\underset{\sim}{R}_j$. These matrix elements represent a gain in energy due to an electron transfer from $\underset{\sim}{R}_i$ to $\underset{\sim}{R}_j$. However, such an electron transfer costs an electrostatic energy

$$U = (e^2/r_{12}) \exp(-\xi r_{12}) \tag{8}$$

where the screening parameter $\xi = \xi(b)$ increases with increasing b_{ij}. Second-order perturbation theory gives the superexchange interaction energy [6, 7]

$$\mathcal{H}_{ex} = -\sum_{ij}\{J_{ij}\underset{\sim}{S}_i \cdot \underset{\sim}{S}_j + \underset{\sim}{D}_{ij}\underset{\sim}{S}_i \times \underset{\sim}{S}_j\} \tag{9}$$

where the dominant contribution to the isotropic exchange parameter is

$$J_{ij} \approx -2b_{ij}^2/U \quad . \tag{10}$$

The minus sign enters because electron transfer conserves the total angular momentum $\underset{\sim}{j} = \underset{\sim}{\ell} + \underset{\sim}{s}$: With half-filled J = 2 states, the Pauli exclusion principle excludes electron transfer between states of parallel spin, and antiferromagnetic coupling is stabilized. Further, the antiferromagnetic ordering temperature is

$$T_N \sim J_{ij} \sim \lambda_\pi^4/U \tag{11}$$

where U decreases with increasing λ_π. The existence of an anisotropic exchange parameter [7]

$$D_{ij} \approx (\Delta g/g)J_{ij} \tag{12}$$

introduces parasitic ferromagnetism, but does not alter Equation (11). Here Δg is the variation of the spectroscopic splitting factor from g = 2. Finally, spin-orbit coupling and collinear spins below T_N order the occupied J = 2 orbitals so as to give a cooperative distortion of a cubic crystal to tetragonal ($c/a < 1$) symmetry [8].

These considerations lead to the following predictions for perovskites containing B cations having two localized outer electrons: At high temperatures the magnetic susceptibility is temperature-dependent; antiferromagnetic order sets in below a T_N that increases sharply with the covalency parameter λ_π; cubic crystals ($\underset{\sim}{D}_{ij} = 0$) have collinear spins and should exhibit a tetragonal ($c/a < 1$) $\rightleftarrows$ cubic transition at T_N whereas orthorhombic crystals having space group Pbnm ($\underset{\sim}{D}_{ij} \neq 0$) may exhibit a parasitic ferromagnetism in the interval $T_t < T < T_N$, where $T_t \leq T_N$ marks an O′-orthorhombic ($c/\sqrt{2} < a \leq b$) $\rightleftarrows$ O-orthorhombic ($a < c/\sqrt{2} < b$) transition as a result of a cooperative spin-orbit-coupling distortion below T_t that orders the principal spin component along the c-axis, making $\underset{\sim}{D}_{ij} = 0$. Electrical conductivity has a semiconducting temperature dependence with an activation energy

$$\epsilon_t = \frac{1}{2} U + \epsilon_a \tag{13}$$

for intrinsic material. Here ϵ_a comes from an activated mobility for localized charge carriers.

As λ_π increases, the interactions become stronger; and for large λ_π the transfer energies of Equation (7) become so large that the assumption of localized electrons breaks down. For large enough λ_π, screening effects make $U \approx 0$ and, in the tight-binding approximation, the width of the allowed energy band is

$$w_b \sim b_{ij} \sim \lambda_\pi^2 \quad . \tag{14}$$

In this limit there is no spontaneous magnetism of the two outer d electrons per B cation, only a temperature-independent Pauli paramagnetism due to a half-filled $J = 3/2$ band. Given a $U = 0$, superconducting diamagnetism should appear below a transition temperature T_{cs}. However, as λ_π decreases, a $U \neq 0$ begins to appear, first quenching T_{cs} [9] and then introducing a temperature-dependent susceptibility χ_m and a splitting in two of the $J = 3/2$ band [10]. The energy gap between the two half-bands is roughly

$$E_g \approx (U^2 + \frac{1}{4} w_b^2)^{\frac{1}{2}} - \frac{1}{2} w_b \quad , \tag{15}$$

and charge-carrier mobilities are not activated ($\epsilon_a = 0$). Where $E_g \neq 0$, further stabilization can be achieved at low temperatures by a spontaneous antiferromagnetic ordering, since this would increase the energy discontinuity about the Fermi energy [11]. Thermal excitation across the gap decreases the stabilization energy due to magnetic

order, and the ordering temperature T_N should decrease with E_g and hence with increasing λ_π.

Figure 2 shows a schematic b_{ij}-T phase diagram, where the electrons are localized for $b_{ij} < b_c$ and spontaneous antiferromagnetism occurs for $b_{ij} < b_m$. Since both b_c and b_m are determined by a critical value of the ratio b_{ij}/U, where U is anticipated from Equation (8) to decrease rapidly with increasing b_{ij}, the critical parameters b_c and b_m should be sharply defined. Finally note that in the collective-electron domain $b > b_c$, any spontaneous crystallographic distortions would be due to our ordering among collective electrons that either increased or introduced an energy discontinuity at the Fermi surface [12]. With an anion intermediary, spontaneous antiferromagnetic order is energetically more favorable than cationic clustering, and no spontaneous crystallographic distortion is anticipated below T_N.

The interval $b_c < b < b_m$ is clearly transitional between the conditions for localized electrons, where crystal-field theory is applicable, and the conditions for $U \approx 0$, where conventional band theory is applicable. It is only in this interval that the difficult problem of correlations among collective electrons must be introduced. It is therefore of great interest to know how extensive this transitional region is, or whether there is a first-order phase change from $b < b_c$ to $b > b_m$, as first suggested by Mott [13] for the case of interactions between impurity centers in doped semiconductors.

Application of the Electronic Phase Diagram

The compounds of Table 2 are listed in the order of decreasing $b_{ij} \sim \lambda_\pi^2$. The argument for this ordering goes as follows: There should be greater λ_π for B cations of larger formal charge (4+ vs 3+) and for 4d orbitals vs 3d orbitals given the same formal charge. Thus λ_π is greater for Mo^{4+} ions than for Cr^{4+} ions, and for Cr^{4+} ions than for V^{3+} ions. Further, the anionic p_π orbitals not only π-bond with the B cations, but also σ-bond with the A cations. This produces a competition for covalent mixing with the anionic p_π orbitals, a competition between the B-cation orbitals of t_{2g} symmetry and the A-cation sp^3 orbitals. The more basic (more ionic) the A cation, the less it competes with the B-cation covalency and hence the larger λ_π. Therefore λ_π increases in the series A = Pb^{2+}, Ca^{2+}, Ba^{2+} and in the series A = Y^{3+}, La^{3+}. The most subtle changes in λ_π should occur within the series $A^{2+}MoO_3$, $A^{2+}CrO_3$, or $A^{3+}VO_3$. The decrease in λ_π on going from $PbCrO_3$ to $LaVO_3$ is primarily due to a reduced B-cationic charge. The larger formal charge on La^{3+} vs Pb^{2+}, which

TABLE 2

Physical Properties of Perovskites with d^2 Configuration at the B Cations

Compound	$T_N(^oK)$	$d\rho/dT$[b]	Symm. 300°K	Remarks	Refs.
$BaMoO_3$	Pauli[a]	> 0	Cubic		15
$SrMoO_3$	Pauli[a]	> 0	Cubic		15
$CaMoO_3$	Pauli[a]	> 0	Ortho.		
$SrCrO_3$	Pauli[a]	> 0	Cubic		3
$CaCrO_3$	90	< 0	Ortho.	$dT_N/dP = -0.23^oK/kbar$	
$PbCrO_3$	240	< 0	Cubic	Collinear Type-G order $T < T_N$	2
$LaVO_3$	137	< 0	(Cubic)	Tet. ($c/a < 1$) ⇄ Cubic at T_N	14
YVO_3	110	< 0	Ortho.	DTA anomaly at $T_t = 73^oK$	14

a. Pauli = temperature-independent χ_m and no spontaneous magnetic order.

b. ρ = electrical resistivity: Metallic ($d\rho/dT > 0$) vs semiconducting ($d\rho/dT < 0$).

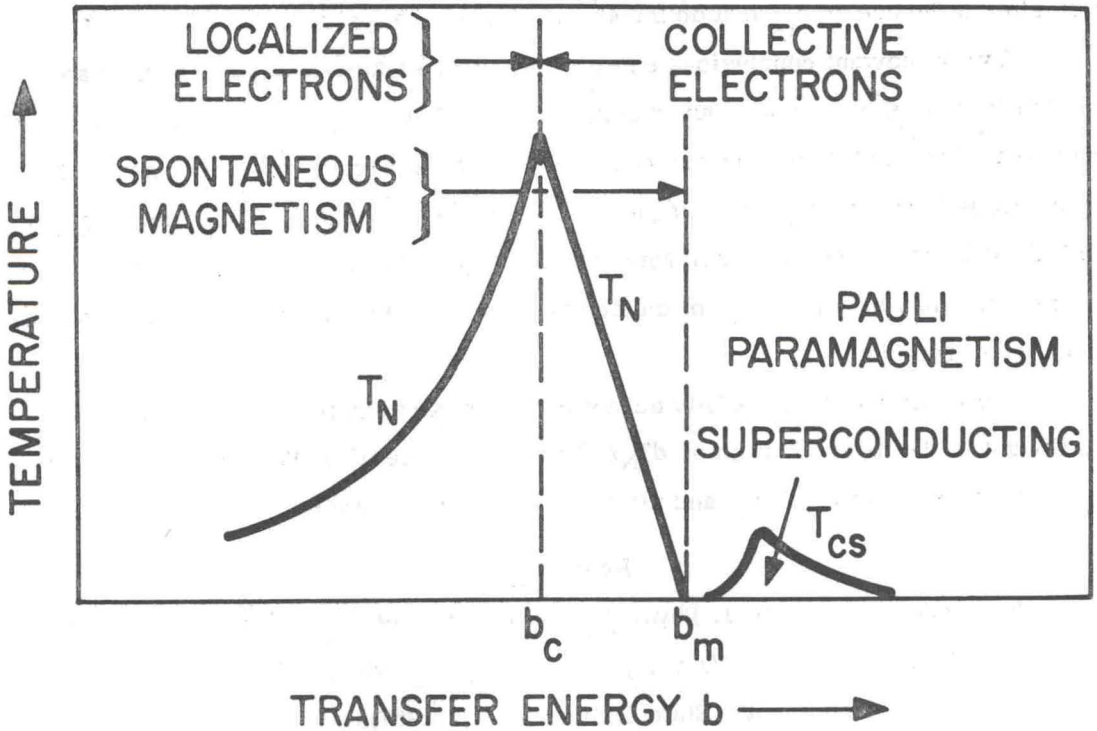

FIG. 2

Electronic phase diagram for one electron per interacting orbital. Semiconducting for $b_{ij} < b_m$, metallic for $b_{ij} > b_m$.

introduces more covalency in the A-O bond, is largely compensated by the fact that lanthanum is far to the left of lead in the periodic table.

Comparison of Table 2 with the phase diagram of Fig. 2 places $SrCrO_3$ and $AMoO_3$ (A = Ca, Sr, Ba) in the domain $b_{ij} > b_m$, $PbCrO_3$ and $CaCrO_3$ in the transitional domain $b_c < b_{ij} < b_m$, and the two vanadates $LaVO_3$, YVO_3 in the localized-electron domain $b_{ij} < b_c$. The fact that $PbCrO_3$ remains cubic to lowest temperatures, even though it has a collinear type-G antiferromagnetic order [2], is consistent with collective d electrons. By contrast, $LaVO_3$ exhibits a tetragonal ($c/a < 1$) to cubic (or O′-orthorhombic to O-orthorhombic, where distrotions toward orthorhombic symmetry are very small) transition [14], which is characteristic of spin-orbit coupling and localized d electrons having collinear spins. YVO_3, which does not undergo a crystallographic transition at T_N, exhibits a definite DTA anomaly at $73^oK < T_N$, which suggests the anticipated O′-orthorhombic to O-orthorhombic transition. Finally, a $dT_N/dP < 0$ for $CaCrO_3$ is consistent with Fig. 2 and $b_c < b_{ij} < b_m$, since b_{ij} should increase with a pressure-induced decreasing lattice parameter. (Changes in the lattice parameter by chemical means, as in $CaCrO_3$ vs $SrCrO_3$, have a smaller influence on b_{ij} than do the accompanying changes in A-O covalency.)

Two important conclusions emerge from these studies: (1) An intermediate domain $b_c < b_{ij} < b_m$ exists, but is quite narrow. The compounds $PbCrO_3$ and $CaCrO_3$ may be said to exhibit spontaneous collective-electron magnetism in contrast to the spontaneous localized-electron magnetism of YVO_3 and $LaVO_3$. (2) The fact that $CaCrO_3$ exhibits parasitic ferromagnetism demonstrates that antisymmetric exchange interactions may be a property of collective-electron magnetism as well as of localized-electron magnetism.

We would like to gratefully acknowledge the participation of N. Menyuk and K. Dwight in the determination of dT_N/dP, the assistance of D. Batson and T. Hilton in the preparation of $CaCrO_3$, and the thermogravimetric analysis by C. Anderson.

References

1. J. B. Goodenough, J. Appl. Phys. 37, 1415 (1966); 39, 403 (1968).
2. W. L. Roth and R. C. DeVries, J. Appl. Phys. 38, 951 (1967).
3. B. L. Chamberland, Solid State Comm. 5, 663 (1967).
4. R. C. DeVries and W. L. Roth, J. Am. Ceramic Soc. 51, 72 (1968).
5. S. Geller and E. A. Wood, Acta Cryst. 9, 563 (1956).

6. P. W. Anderson, Phys. Rev. 115, 2 (1959).

7. T. Moriya, Phys. Rev. 120, 91 (1960).

8. J. B. Goodenough (unpublished research).

9. N. F. Berk and J. R. Schrieffer, Phys. Rev. Lett. 17, 433 (1966).

10. J. Hubbard, Proc. Royal Soc. (London) A276, 238 (1964).

11. J. C. Slater and G. F. Koster, Phys. Rev. 94, 1498 (1964).

12. J. B. Goodenough, Mater. Res. Bull. 2, 37, 165 (1967).

13. N. F. Mott, Can. J. Phys. 34, 1356 (1956).

14. D. B. Rogers, A. Ferretti, D. H. Ridgley, R. J. Arnott and J. B. Goodenough, J. Appl. Phys. 37, 1431 (1966).

15. L. H. Brixner, J. Inorg. Nucl. Chem. 14, 225 (1960).